This article has been accepted for publication in a future issue of this journal, but has not been fully edited. Content may change prior to final publication. Citation information: DOI 10.1109/TPEL.2018.2878967, IEEE Transactions on Power Electronics

A new pulse active width modulation (PAWM) for multilevel converters

Concettina Buccella *Senior Member, IEEE,* Maria Gabriella Cimoroni, Mario Tinari, Carlo Cecati *Fellow, IEEE*

***Abstract*—This paper proposes a new pulse amplitude width modulation (PAWM) procedure for cascaded H-bridges multilevel inverters fed by DC voltage sources with unequal amplitudes. With proposed procedure, the generated output voltage is obtained modulating a sinusoidal reference signal at the desired fundamental frequency with equally spaced switching angles. It has been analytically demonstrated that, under these assumptions, all harmonics except those of order $n = 2kl \pm 1$, $k = 1, 2, \ldots$ are deleted from the output voltage waveform. After a detailed description of the method and a comparative analysis with others existing in literature, its harmonics elimination capability has been experimentally verified with 5, 7, 9 and 11 level cascaded H-bridge inverters, moreover it has been mathematically demonstrated that it reduces THD below 5% with a 17-level inverter and it is capable to eliminate the first 49 harmonics considered by standards with a 27-level inverter.**

***Index Terms*—Total Harmonic Distortion (THD), Pulse Active Width Modulation (PAWM), Multilevel Inverters, Selective Harmonics Elimination (SHE), Selective Harmonics Mitigation (SHM).**

I. Introduction

Because of their topology, cascaded H-bridge (CHB) multilevel converters can successfully operate with fundamental or low frequency as well as with pulse width modulation, offering significantly better output waveforms, medium voltage capabilities and often better efficiency than conventional two-level converters. Selective harmonic elimination (SHE) modulation methods are quite popular in high power multilevel converters because while eliminating predefined low order harmonics, they are capable to maintain the fundamental voltage at the desired level [1]- [2]. SHE methods can be classified in SHE-pulse-width modulation (SHE-PWM) e.g. [1]- [3] and SHE-pulse-amplitude modulation (SHE-PAM) [4]- [5]. Considering recent relevant papers only, [6] applies SHE technique to 7-levels cascaded multilevel inverters to eliminate third and fifth harmonics when the modulation index ranges between 0.1 and 1.04, [7] presents a modified SHE-PWM method which improves the output voltage of a 5-level inverter operating in a wide modulation index range. Usually, SHE-PWM methods consider the switching angles as the unique degrees of freedom. For an assigned number of levels and a PWM algorithm, the number of eliminated harmonics is strictly related to the number of switching angles, therefore, while increasing the number of commutations, the harmonic content decreases, but at the cost of increased switching losses. SHE-PAM techniques overlap pulse width modulation with input voltage amplitude variations, therefore the degrees of freedom increases. The mathematical problem is usually reformulated such as to keep constant the switching angles within a wide modulation index range. Unequal DC link voltages and dynamic voltage unbalances are significant issues with multilevel converters. To face with them, some modulation methods have been proposed, such as the elimination theory and the concept of resultants, described in [8] or the Particle Swarm Optimization (PSO) theory [9] and the Homotopy [10]. Paper [11] presents a multilevel selective harmonic elimination pulse-width modulation (MSHE-PWM) technique for transformerless static synchronous compensators (STATCOM) optimizing both DC-voltage levels and switching angles, [12] proposes a SHE algorithm for a 5-level cascaded inverter operating at fundamental frequency, based on graphical separation of functions zeros, [13] presents a SHE-PWM fullfilling IEC 61000-3-6, IEC 61000-2-12, EN 50160 and CIGRE WG 36-05 standards for single and three phase medium voltage H-bridge converters with variable DC links. Paper [14] proposes a generalized formulation of a selective harmonic mitigation pulse amplitude modulation (SHM-PAM) useful to control CHB inverters with unequal DC sources. Usually, SHE algorithms require the solution of a mathematical system with transcendental equations, bounded within the full range of modulation indices or operating points. Proposed iterative techniques such as Newton—-Raphson, sequential quadratic programming, gradient optimisation, theory of resultants are computationally burdensome and often subject to convergence problems, particularly when the number of variables increases. Among some others, a Groebner-based SHE-PWM algebraic method has been proposed in [15] and [16]: the nonlinear and high-order SHE equations are converted in an equivalent triangular form, then a recursive algorithm has been used to solve each triangular equation. Fast and accurate analitycal methods have been presented in [17] and [18], both for a 5-level inverter. It is worth notice that none of these methods provides switching states for continuously varying operating point applications. This paper presents a pulse active width modulation (PAWM) characterized by equally-spaced switching angles. It has been developed for l-level CHB inverters fed by s unequal DC voltage sources. Adopting proposed method, all harmonics, except those of order $n = 2kl \pm 1$, $k = 1, 2, \ldots$ disappear from the output voltage. Its modulation index is bounded within the range $0 \leq m \leq 1$, were closed solutions always exist. A

C. Buccella, M.G. Cimoroni, M. Tinari and C. Cecati are with the Department of Information Engineering, Computer Science and Mathematics, University of L'Aquila and with DigiPower srl, L'Aquila, Italy, e-mails: name.family_name@univaq.it

This article has been accepted for publication in a future issue of this journal, but has not been fully edited. Content may change prior to final publication. Citation information: DOI 10.1109/TPEL.2018.2878967, IEEE Transactions on Power Electronics

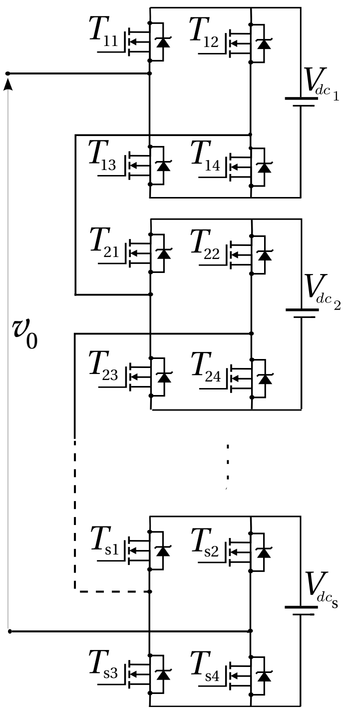

Fig. 1. Multilevel inverter configuration.

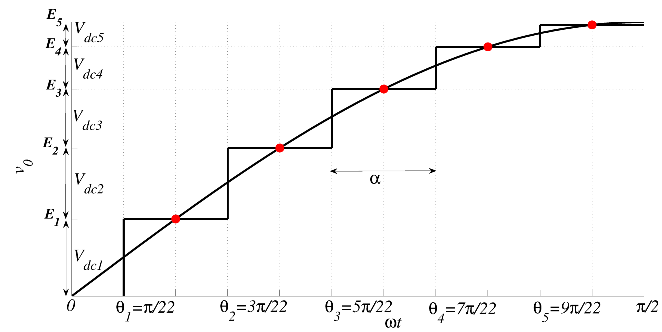

Fig. 2. 11-level inverter output voltage waveform.

mathematical proof of the number and the order of deleted harmonics is given and some experimental results have been included for validation purposes. It is worth notice that with proposed method neither switching angles or output voltage total harmonic distortion (THD) depend on the modulation index m, which can be easily modified changing DC voltage levels. Proposed method can be successfully adopted in all those applications adopting variable DC sources, such as photovoltaic energy systems, uninterruptible power supplies (UPS), electric vehicle powertrains, etc. The advantages and feasibility of the proposed PAWM have been evaluated through comparative analysis with the methods described in [4], [5], [13], [14], [17]- [20].

II. Pulse active width modulation (PAWM)

A l-level cascaded inverter, consisting of s H-bridges fed by s unequal DC voltage sources V_{dc1}, V_{dc2}, ... , V_{dcs}, has been considered, as shown in Fig. 1. Assuming the following hypotheses:

1) the output voltage waveform v_0 is modulated by a reference sinusoidal signal (RSS) at fundamental frequency
2) the switching angles are chosen as $\theta_k = (2k-1)\frac{\pi}{2l}, \quad k = 1,\ 2\ldots,\ s$ and are equispaced with step $\alpha = \frac{\pi}{l}$, $l = 2s+1$ within the interval $\left[0,\ \frac{\pi}{2}\right]$
3) the output v_0, consists of s levels E_1, E_2, ... E_s calculated in the following manner: considering a generic interval $[\theta_k,\ \theta_{k+1}]$, the level E_k is fixed at the magnitude of the RSS in the middle point, given by:

$$E_k = V_m \sin\left(\frac{\theta_k + \theta_{k+1}}{2}\right) = V_m \sin(k\alpha) \quad k = 1,\ 2, ...,\ s \quad (1)$$

where V_m is the peak value of the RSS (see Fig.2).

The amplitudes of the DC voltage sources are:

$$V_{dck} = E_k - E_{k-1} \qquad k = 1,\ 2, ...,\ s \qquad (2)$$

with $E_0 = 0$ and $\theta_{s+1} = \frac{\pi}{2}$.

Under these assumptions and applying the Fourier series expansion, the amplitude of the n^{th} harmonic V_n of v_0 is given by:

$$V_n = \frac{4}{n\pi} \sum_{k=1}^{s} (E_k - E_{k-1}) \cos(n\theta_k) \qquad (3)$$

Because v_0 is an odd function, even harmonics are absent and (3) holds only for odd harmonics.

Just to examplify, a 11-level inverter is considered in Fig. 2. In this case, $s = 5$, $l = 11$, $\theta_1 = \frac{\pi}{22}$, $\theta_2 = \frac{3\pi}{22}$, $\theta_3 = \frac{5\pi}{22}$, $\theta_4 = \frac{7\pi}{22}$ and $\theta_5 = \frac{9\pi}{22}$. The amplitude of the first harmonic must be set equal to the modulation index value.

Rearranging (3), follows:

$$V_n = \frac{4}{n\pi} \sum_{k=1}^{s} E_k \left[\cos\left(n(2k-1)\frac{\alpha}{2}\right) - \cos\left(n(2k+1)\frac{\alpha}{2}\right)\right] \qquad (4)$$

The term $\cos\left((2s+1)n\frac{\alpha}{2}\right) = 0$ because when n is odd then $(2s+1)n\frac{\alpha}{2} = n\frac{\pi}{2}$.

Applying Prosthaphaeresis formula in (4) and substituting E_i with (1), follows:

$$V_n = \frac{4 \cdot 2V_m}{n\pi} \sin\left(n\frac{\alpha}{2}\right) \left[\sum_{k=1}^{s} \sin(nk\alpha)\sin(k\alpha)\right] \qquad (5)$$

After some goniometric manipulations, follows:

$$V_n = \frac{4 \cdot V_m}{n\pi} \sin\left(n\frac{\alpha}{2}\right) \sum_{k=1}^{s} [\cos((n-1)k\alpha) + - \cos((n+1)k\alpha)]. \qquad (6)$$

III. Analytical computation of the n values giving $V_n = 0$ for a variable l

This Section aims at demonstrating that proposed modulation technique eliminates all harmonics, except those of order $n = 2kl \pm 1$, $k = 1,\ 2, \ldots$. The case $n = -1$ is not significant for the considered applications. Notice that in (6) the term $\sin\left(n\frac{\alpha}{2}\right)$ is equal to zero only if the term $n = 2kl$ is even,

This article has been accepted for publication in a future issue of this journal, but has not been fully edited. Content may change prior to final publication. Citation information: DOI 10.1109/TPEL.2018.2878967, IEEE Transactions on Power Electronics

hence, only the sum $\sum_{k=1}^{s}\left[\cos\left((n-1)\,k\alpha\right)-\cos\left((n+1)\,k\alpha\right)\right]$ contributes to the computation of n giving $V_n=0$ [21].

Theorem 1. *The sum*

$$\sum_{k=1}^{s}\left[\cos\left((n-1)\,k\alpha\right)-\cos\left((n+1)\,k\alpha\right)\right] \tag{7}$$

$\alpha=\frac{\pi}{l},\ \ l=2s+1,\ \ s=2,\ 3,\ \ldots$
is equal to zero for all odd n*,* $n\neq 2kl\pm 1,\ k=0,\ 1,\ 2,\ \ldots$.

Proof: Introducing the function $S_l\left(h\right)$

$$S_l\left(h\right)=\sum_{k=1}^{s}\cos\left(hk\alpha\right) \tag{8}$$

with $h=n\pm 1$ and applying Eulero's formula to (8), the following expression is obtained:

$$S_l\left(h\right)=\frac{1}{2}\left[\sum_{k=1}^{s}\left(e^{ih\alpha}\right)^k+\sum_{k=1}^{s}\left(e^{-ih\alpha}\right)^k\right] \tag{9}$$

with i imaginary unit. Since the sums in (9) are geometrical, (10) is obtained as:

$$S_l\left(h\right)=\frac{1}{2}\left[e^{ih\alpha}\frac{1-e^{ih\alpha s}}{1-e^{ih\alpha}}+e^{-ih\alpha}\frac{1-e^{-ih\alpha s}}{1-e^{-ih\alpha}}\right] \tag{10}$$

$h\neq 2kl,\ k=0,\ 1,\ 2,\ \ldots$.
After some mathematical manipulations (see Appendix), follows:

$$S_l\left(h\right)=\frac{\sin\left(h\frac{\pi}{4}\ \frac{l-1}{l}\right)}{\sin\left(h\frac{\pi}{2l}\right)}\cos\left(h\frac{\pi}{4}\ \frac{l+1}{l}\right) \tag{11}$$

with $h\neq 2lk,\ k=0,1,2,\ldots$. Rearranging (11) by using goniometric formulas, the following relationship can be obtained:

$$S_l\left(h\right)=\frac{1}{2}\left[\frac{\sin\left(h\frac{\pi}{2}\right)}{\sin\left(h\frac{\pi}{2l}\right)}-1\right] \tag{12}$$

From (8) and (12), the sum (7) becomes:

$$\begin{aligned}&\sum_{k=1}^{s}\left[\cos\left((n-1)\,k\alpha\right)-\cos\left((n+1)\,k\alpha\right)\right]=\\&=S_l\left(n-1\right)-S_l\left(n+1\right)=\\&\frac{1}{2}\left[\frac{\sin\left((n-1)\frac{\pi}{2}\right)}{\sin\left((n-1)\frac{\pi}{2l}\right)}-\frac{\sin\left((n+1)\frac{\pi}{2}\right)}{\sin\left((n+1)\frac{\pi}{2l}\right)}\right]\end{aligned} \tag{13}$$

and, after easy mathematical manipulations, the following relationship can be obtained:

$$\begin{aligned}&\sum_{k=1}^{s}\left[\cos\left((n-1)\,k\alpha\right)-\cos\left((n+1)\,k\alpha\right)\right]=\\&=-\cos\left(n\frac{\pi}{2}\right)\frac{\cos\left(\frac{\pi}{2l}\right)\sin\left(n\frac{\pi}{2l}\right)}{\sin\left((n-1)\frac{\pi}{2l}\right)\sin\left((n+1)\frac{\pi}{2l}\right)}\end{aligned} \tag{14}$$

For n odd, $n\neq 2lk\pm 1,\ k=0,\ 1,\ 2,\ \ldots$, (14) is zero.
In order to evaluate (14) in $n=2lk\pm 1$, where it is not defined (because has the form $\frac{0}{0}$), the application of the De L'Hospital rule leads to:

$$\begin{aligned}&\lim_{n\to 2lk\pm 1}\left[-\cos\left(\frac{\pi}{2l}\right)\cos\left(n\frac{\pi}{2}\right)\right.\\&\left.\frac{\sin\left(n\frac{\pi}{2l}\right)}{\sin\left((n-1)\frac{\pi}{2l}\right)\sin\left((n+1)\frac{\pi}{2l}\right)}\right]=\pm\frac{l}{2}\end{aligned} \tag{15}$$

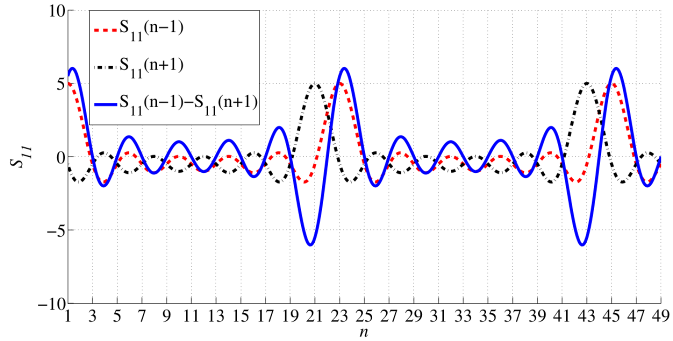

Fig. 3. Behaviour of the functions $S_{11}\left(n-1\right)$, $S_{11}\left(n+1\right)$ and their difference.

Therefore, it is demonstated that for $n=2lk\pm 1$, the sum $\sum_{k=1}^{s}\left[\cos\left((n-1)\,k\alpha\right)-\cos\left((n+1)\,k\alpha\right)\right]\neq 0$.
From (14) and (15), the thesis is demostrated. ■

Just to include an example, a 11-level inverter is considered here. Fig. 3 shows the functions $S_{11}\left(n-1\right)$, $S_{11}\left(n+1\right)$ and their difference, highlighting that only the harmonics with order $n=21,\ 23,\ 43,\ 45$ are not zero. Fig. 4 shows the effect of the modulation index m on the switching angles and on the DC voltage sources. It can be observed that the switching angles remain constant while the DC voltage varies linearly with m.
Fig. 5 shows the harmonic analysis obtained for l-level CHB inverters with $l=5,\ 7,\ 9,\ 11,\ 13,\ 15$.

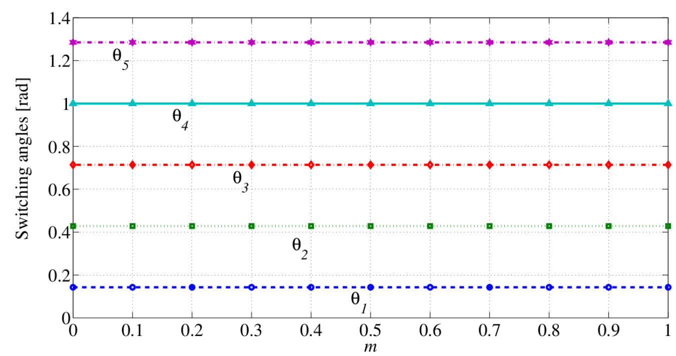

(a) switching angles

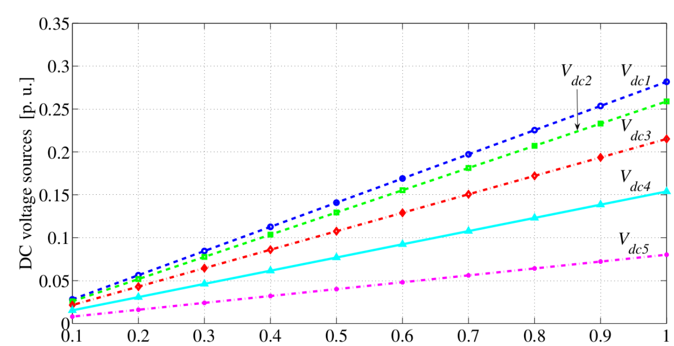

(b) DC voltage sources with m

Fig. 4. Variations in 11-level CHB inverter.

This article has been accepted for publication in a future issue of this journal, but has not been fully edited. Content may change prior to final publication. Citation information: DOI 10.1109/TPEL.2018.2878967, IEEE Transactions on Power Electronics

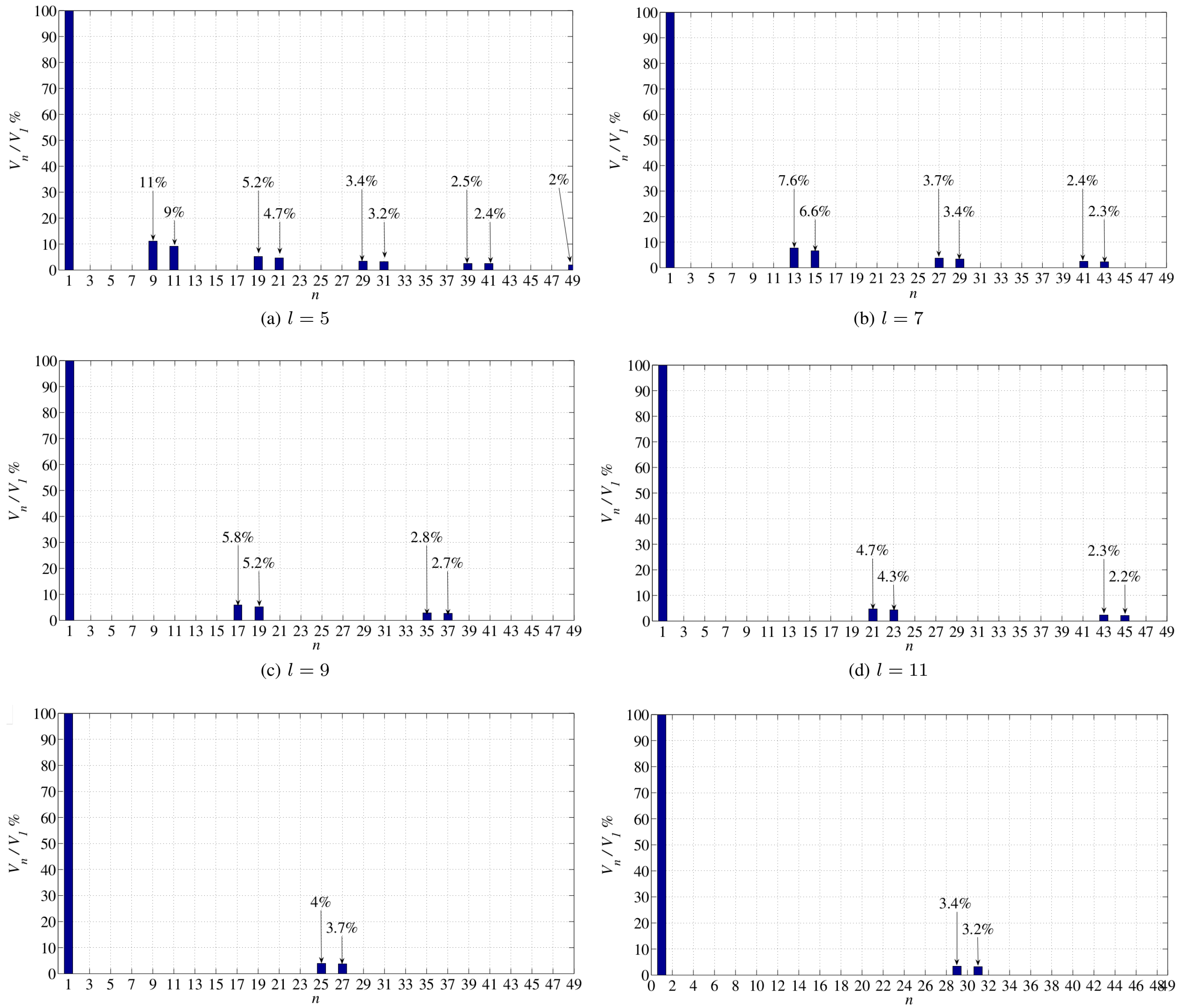

(a) $l = 5$ (b) $l = 7$

(c) $l = 9$ (d) $l = 11$

(e) $l = 13$ (f) $l = 15$

Fig. 5. Harmonic analysis in a l-level CHB inverter.

IV. Comparison with other modulation techniques

In order to demonstate the quality of PAWM, it has been compared with some methods already proposed in literature.

A. Comparison with the method described in [5]

The method proposed in [5] has been implemented and compared with PAWM. It has been found that proposed method cancels more harmonics than the one in [5] but it does not delete the harmonics having order:

$$2lk \pm 1 \qquad k = 1,\, 2,\, \ldots \tag{16}$$

On the other side, the procedure in [5] does not delete the harmonics having order:

$$2Lk \pm 1 \; k = 1,\, 2,\, \ldots \tag{17}$$

where $L = l - 1$, therefore:

$$2\,(l-1)\,k \pm 1 = 2lk \pm 1 - 2k \quad k = 1,\, 2,\, \ldots\, . \tag{18}$$

Comparing (16) with (18) the term $2k$ implies that in [5] the first not deleted harmonic (for $k = 1$) has order $(2l - 3)$ which is lower than the order $(2l - 1)$ obtained by PAWM. For exaple for a 5-level inverter and considering up to the 49^{th} harmonic, PAWM does not cancel 9 harmonics, but the procedure in [5] doesn't delete 12 harmonics (see Table I).

It can be noted that in PAWM the first switching angle is always different by zero: in fact, the switching angles are chosen such as $\theta_k = (2k-1)\,\frac{\pi}{2l}$, $\quad k = 1, .2.., s$. In [5], the first angle is always equal to zero: in fact, the angles are chosen such as $\theta_k = (k-1)\,\frac{\pi}{(l-1)}$, $\quad k = 1, .2.., s$ (see formula (5) in [5]). Table I summarizes, for multilevel inverters with

This article has been accepted for publication in a future issue of this journal, but has not been fully edited. Content may change prior to final publication. Citation information: DOI 10.1109/TPEL.2018.2878967, IEEE Transactions on Power Electronics

$l = 5, 7, 9, 11, 13$ and considering up to 49^{th} harmonic, the harmonics deleted by PAWM and by the technique in [5]. The red dots represent the not-canceled harmonics with PAWM, the blu dots the not-canceled harmonics with modulation in [5]; the 'x' symbols represent the deleted ones.

The THD% of the output voltage is defined as:

$$\mathrm{THD}\% = \frac{\sqrt{\sum_{i=3,5\ldots}^{49} V_i^2}}{V_1} 100 \tag{19}$$

and it is constant while the modulation index varies. Fig. 6 shows the output voltage THD% for the considered modulations applied to an inverter with the number of levels up to $l = 21$. The better performance of PAWM over [5] is evident.

TABLE I
COMPARISON BEETWEEN PAWM AND THE TECHNIQUE IN [5].

	l									
	5		7		9		11		13	
n	PAWM	[5]	PAWM	[5]	PAWM	[5]	PAWM	[5]	PAWM	[5]
3	x	x	x	x	x	x	x	x	x	x
5	x	x	x	x	x	x	x	x	x	x
7	x	●	x	x	x	x	x	x	x	x
9	●	●	x	x	x	x	x	x	x	x
11	●	x	x	●	x	x	x	x	x	x
13	x	x	●	●	x	x	x	x	x	x
15	x	●	●	x	x	●	x	x	x	x
17	x	●	x	x	●	●	x	x	x	x
19	●	x	x	x	●	x	x	●	x	x
21	●	x	x	x	x	x	●	●	x	x
23	x	●	x	●	x	x	●	x	x	●
25	x	●	x	●	x	x	x	x	●	●
27	x	x	●	x	x	x	x	x	●	x
29	●	x	●	x	x	x	x	x	x	x
31	●	●	x	x	x	●	x	x	x	x
33	x	●	x	x	x	●	x	x	x	x
35	x	x	x	●	●	x	x	x	x	x
37	x	x	x	●	●	x	x	x	x	x
39	●	●	x	x	x	x	x	●	x	x
41	●	●	●	x	x	x	x	●	x	x
43	x	x	●	x	x	x	●	x	x	x
45	x	x	x	x	x	x	●	x	x	x
47	x	●	x	x	x	●	x	x	x	●
49	●	●	x	●	x	●	x	x	x	●

B. Comparison of PAWM with conventional SHE-SHM-PWM and SHE-SHM-PAM methods

In this subsection, the performance of proposed PAWM has been compared with those of some implementations of conventional SHE-SHM-PWM: [17], [18], [19], [20] and of SHE-SHM-PAM: [4], [13], [14]. One switching transition has been considered per each level, which leads to identical switching frequency in SHE-SHM methods. Conventional

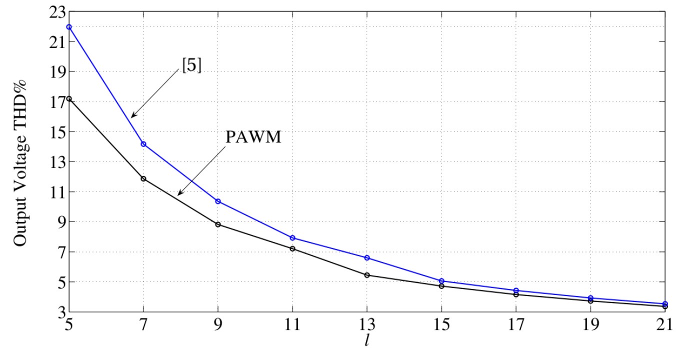

Fig. 6. Comparison between output voltage THDs% at different number of levels.

SHE-PWM and SHE-PAM eliminate a total number of $\frac{l-3}{2}$ and $l - 2$ harmonics, respectively. Fig. 7 shows, for the proposed PAWM and for the considered conventional SHE-PWM and SHE-PAM, the number of deleted harmonics as a function of the number of levels. The analysis has been carried out considering up to the 301^{th} harmonic. PAWM eliminates a larger number of harmonics than conventional SHE methods. For example, considering a single phase, 13-level CHB inverter, the total number of harmonics eliminated by SHE-PWM, SHE-PAM and PAWM are 5, 11, 127, respectively; considering a three phase inverter, the total number of harmonics eliminated are 5, 11, 86, respectively.

In the following, three phase systems, have been considered. Since the third and multiple harmonics are intrinsically eliminated, they should not be controlled. The output voltage THD% in 5- and 7- level three phase inverters have been computed and results are shown in Figs. 8a and 8b, respectively. Simulations have been carried out using PAWM and SHM-PAM in [13], [14] to mitigate harmonics with order $k = 5, 7, \ldots, 49$ and SHE-PWM in [17]–[20] to eliminate the fifth harmonic in 5-level inverters, and the fifth and the seventh harmonics in 7-level inverters. Regarding SHE-PWM, if for an assigned m multiple solutions exist, then, the graph in Fig. 8a refers to the values returning the lower THD. It has been found that, for a 7- level inverter the SHE-PWM solution exists only if $m = [0.5, 0.84]$. Fig. 9 shows that, due to the intrinsic elimination of the third and multiple harmonics in three phase systems, adopting 5- and 9- level inverters, proposed PAWM

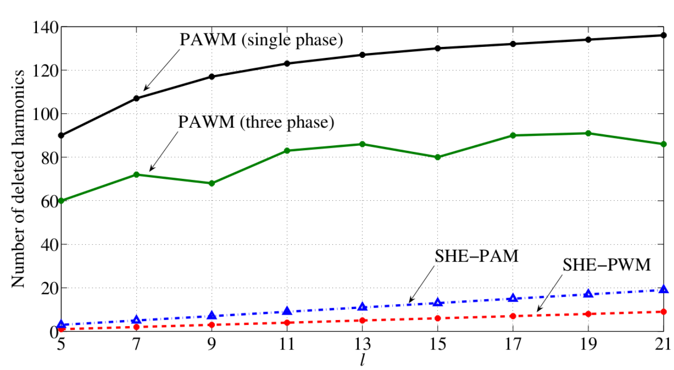

Fig. 7. Number of deleted harmonics as function of number of levels.

This article has been accepted for publication in a future issue of this journal, but has not been fully edited. Content may change prior to final publication. Citation information: DOI 10.1109/TPEL.2018.2878967, IEEE Transactions on Power Electronics

gives a little bit higher THD% than SHM-PAM, but PAWM outperforms SHM-PAM with 7- and and 11-level inverters. The weighted THD (WTHD), i.e. the harmonics amplitudes weighted with respect to the fundamental $\left(\frac{V_n}{V_1}\%\right)$ shown in Fig. 10 is computed for a three phase CHB 5-level inverter modulated by PAWM, by SHE-PWM for the fifth harmonic elimination and considering $m = 0.8$ [17] and by SHM-PAM used to mitigate the harmonics of order $k = 5, 7, \ldots, 49$ [13], [14].

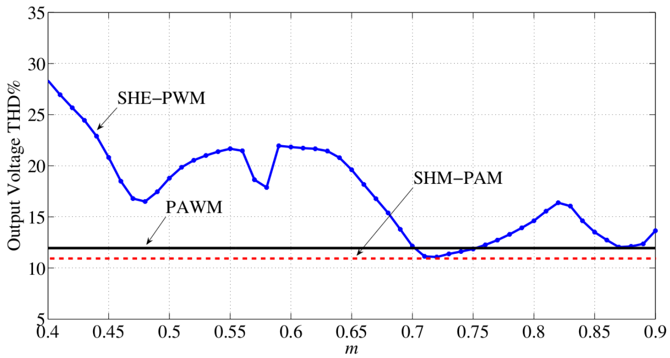

(a) 5-level inverter

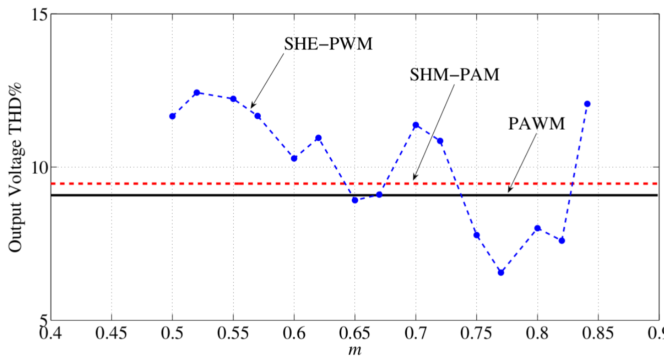

(b) 7-level inverter

Fig. 8. Output voltage THD% obtained with PAWM, SHE-PWM and SHM-PAM.

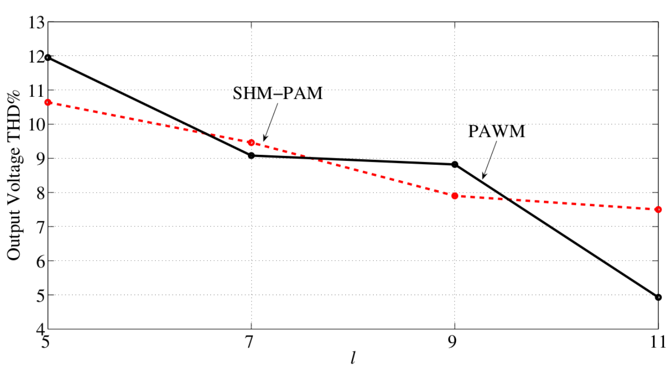

Fig. 9. Output voltage THD% at different levels with PAWM and SHM-PAM.

V. Experimental results

Experimental results have been obtained using 5-, 7-, 9- and 11- level single phase inverters realized cascading H-bridge cells produced by DigiPower srl and rated 600 V, 40

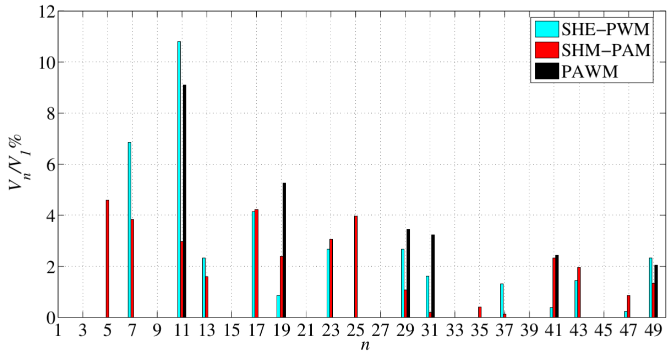

Fig. 10. Weighted THD of a three phase 5-level CHB inverter with PAWM, SHE-PWM and SHM-PAM.

A each [22]. Fig. 11 shows the 9-level inverter configuration. Each cell can operate at switching frequency exceeding 40 kHz and has its own DSP which provides to data acquisition, signal conditioning and calculations, moreover, it includes serial peripheral communication (SPI) channels. The whole multilevel converter is controlled by a field programmable gate array (FPGA) Intel Cyclone®V model SE 5CSEBA6U23I7, programmed using Quartus® [23]- [24]. In this application, the FPGA is in charge of pulse generation with 32-bit resolution and implements interlock logic with dead-band. Modulation patterns are transmitted to the H-bridges through SPI channels. Each H-bridge is supplied according to (2) with $V_m = 380$ V at fundamental frequency 50 Hz using a programmable DC power supply model Lambda - Genesys 600-2.6, rated 600 V, 2.6 A. The load connected to the output terminals has $R = 315\,\Omega$ and $L = 11.56\,\text{mH}$.

An eight channel Digital Oscilloscope Yokogawa DLM4058 (2.5 GS/s 500 MHz) and a three phase power meter Yokogawa WT1800 complete the experimental setup.

Figures 12-13 show obtained results, which are in full agreement with previous theoretical analysis.

Fig. 11. Experimental setup.

The robustness of PAWM to disturbances around the designed DC link voltages, is verified considering a 7-level inverter connected with the RL load.

Assuming the designed DC voltages equal to $V_{dc1r} = 164.9\,V$, $V = 132.2\,V$, $V_{dc3r} = 73.38\,V$, the tests named

This article has been accepted for publication in a future issue of this journal, but has not been fully edited. Content may change prior to final publication. Citation information: DOI 10.1109/TPEL.2018.2878967, IEEE Transactions on Power Electronics

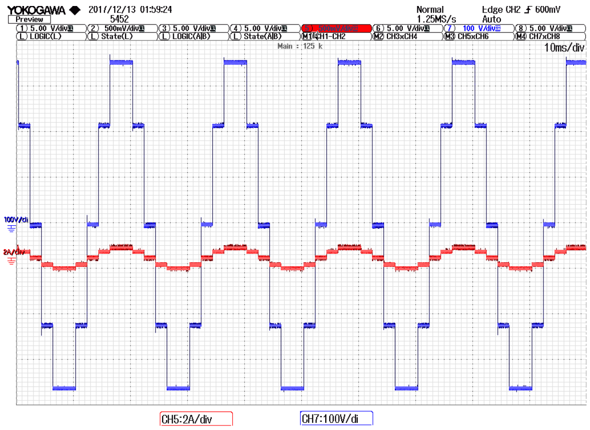

(a) Output voltage (blu line) and current (red line) waveforms

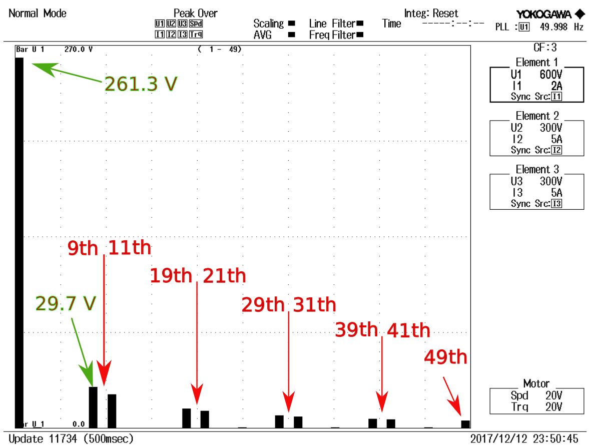

(b) Harmonics amplitudes of output voltage in Volt

Fig. 12. Experimental results in a 5-level inverter.

Case#1, Case#2 and Case#3, during which the considered disturbances are applied, are executed and the corresponding output voltages THD% are measured. Table II summarizes both the applied disturbances and the corresponding THD%. It can be noticed that, during the worst Case#3, THD% increases approximately the same percentage of the DC voltages disturbances, therefore the system is well conditioned. In the best Case#1, the increase of THD% is lower than disturbances percentages.

TABLE II
OUTPUT VOLTAGE THD% VS. DESIGNED DC LINK VOLTAGES DISTURBANCES.

Case	V_{dc1} [V]	V_{dc2} [V]	V_{dc3} [V]	THD%
	V_{dc1r}=164.9	V_{dc2r}=132.2	V_{dc3r}=73.38	11.86
#1	V_{dc1r}-10%=148.4	V_{dc2r}+10%=145.4	V_{dc3r}+5%=77.1	12.32
#2	V_{dc1r}-20%=131.9	V_{dc2r}+20%=158.7	V_{dc3r}+10%=80.7	13.51
#3	V_{dc1r}-30%=115.4	V_{dc2r}+30%=171.9	V_{dc3r}+20%=66.1	15.46

The same 7-level configuration with the same load has been used to evaluate transient conditions during modulation index variations, the latter obtained modifying, for each module, the equation (2), i.e. V_{dck}, $k = 1, 2, 3$. DC voltages values change from $V_{dc1} = 108.5\,\text{V}$, $V_{dc2} = 87\,\text{V}$, $V_{dc3} = 48.3\,\text{V}$ corresponding to $m = 0.657$ to the new values $V_{dc1} = 164.9\,V$, $V_{dc2} = 132.2\,\text{V}$, $V_{dc3} = 73.38\,V$ corresponding to $m = 1$ (see Fig. 14(a)). Voltage and current transient responses are shown in Fig. 14(b). It can be noticed that the steady state condition is reached after about 30 ms.

VI. CONCLUSIONS

A new procedure based on pulse amplitude width modulation (PAWM) has been developed for cascaded H-bridge converters fed by unequal DC voltage sources. Proposed procedure identifies equally spaced switching angles and performs a modulation of the output voltage on the base of a reference sinusoidal signal fixed at the fundamental frequency. A mathematical proof has been presented demonstrating that PAWM deletes all harmonics embedded within the output voltage waveform of a l-level inverter, except those of order $n = 2kl \pm 1$, $k = 1, 2, \ldots$.

Harmonic elimination capability of PAWM in single and three phase cascaded multilevel inverters has been validated by simulation and experimental results as well as by comparisons with some methods described in literature. The main features of PAWM can be summarized as follows:

- high efficiency, obtained due to fundamental switching frequency operations
- more harmonics eliminated than using other methods: for a chosen number of levels and for the whole modulation index range ($0 \le m \le 1$) it fixes, in optimal way, both the switching angles as well as the amplitudes of the DC-voltages
- THD% does not depend on the modulation index
- main grid code requirement fullfilment (THD% < 5%) without any passive filter using a 17- level inverter
- full harmonics elimination (up to 49-th order) using a 27-level inverter.

Applications of PAWM are numerous as it can be successfully implemented on multilevel converters with DC/DC converter front-end, among the others: photovoltaic and wind generators and UPS.

APPENDIX

Formula (10) can be written as:

$$S_l\left(h\right) = \frac{1}{2}\left[e^{ih\alpha}\frac{1-e^{ih\alpha s}}{1-e^{ih\alpha}} + \frac{1}{e^{ih\alpha}}\frac{1-\frac{1}{e^{ih\alpha s}}}{1-\frac{1}{e^{ih\alpha}}}\right] =$$

$$= \frac{1}{2}\left[e^{ih\alpha}\frac{1-e^{ih\alpha s}}{1-e^{ih\alpha}} + \frac{1}{e^{ih\alpha s}}\frac{1-e^{ih\alpha s}}{1-e^{ih\alpha}}\right] =$$

$$= \frac{1}{2}\frac{1-e^{ih\alpha s}}{1-e^{ih\alpha}}\left(e^{ih\alpha} + \frac{1}{e^{ih\alpha s}}\right) =$$

$$= \frac{1}{2}\frac{1-e^{ih\alpha s}}{1-e^{ih\alpha}}\left(\frac{e^{ih\alpha(s+1)}+1}{e^{ih\alpha s}}\right) =$$

$$= \frac{e^{-ih\alpha\frac{s}{2}} - e^{ih\alpha\frac{s}{2}}}{e^{-ih\frac{\alpha}{2}} - e^{ih\frac{\alpha}{2}}}\,\frac{e^{ih\alpha\frac{s}{2}}}{e^{ih\frac{\alpha}{2}}}\,\frac{e^{ih\alpha\frac{s+1}{2}} + e^{-ih\alpha\frac{s+1}{2}}}{2}\,\frac{e^{ih\alpha\frac{s+1}{2}}}{e^{ih\alpha s}} =$$

This article has been accepted for publication in a future issue of this journal, but has not been fully edited. Content may change prior to final publication. Citation information: DOI 10.1109/TPEL.2018.2878967, IEEE Transactions on Power Electronics

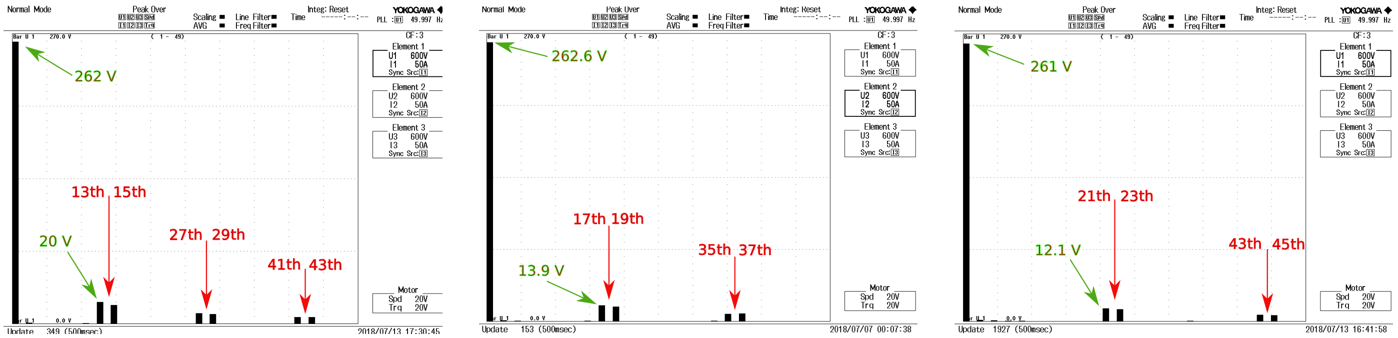

(a) 7-level inverter (b) 9-level inverter (c) 11-level inverter

Fig. 13. Harmonics amplitudes of output voltage.

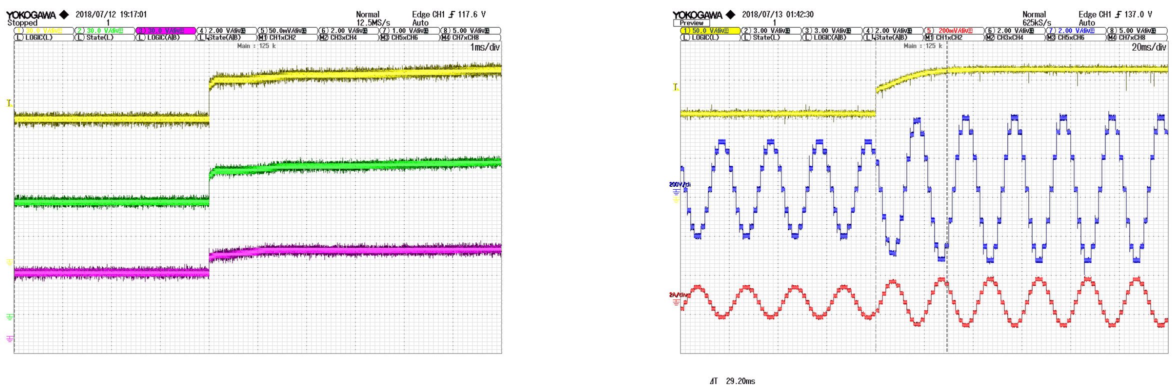

(a) DC voltage sources step to vary modulation index from m=0.64 to m=1

(b) Output voltage (blu line) and current (red line) waveforms

Fig. 14. Transient response.

$$= \frac{\sin\left(h\alpha \frac{s}{2}\right)}{\sin\left(h\frac{\alpha}{2}\right)} \cos\left(h\alpha \frac{s+1}{2}\right) \frac{e^{ih\alpha\frac{s+1}{2}}\, e^{ih\alpha\frac{s}{2}}}{e^{ih\alpha s}\, e^{ih\frac{\alpha}{2}}}.$$

Since $\frac{e^{ih\alpha\frac{s+1}{2}}\, e^{ih\alpha\frac{s}{2}}}{e^{ih\alpha s}\, e^{ih\frac{\alpha}{2}}} = e^{ih\alpha 0} = 1$, previous equation becomes:

$$\frac{\sin\left(h\alpha \frac{s}{2}\right)}{\sin\left(h\frac{\alpha}{2}\right)} \cos\left(h\alpha \frac{s+1}{2}\right) =$$

$$= \frac{\sin\left(h\frac{\pi}{4}\frac{l-1}{l}\right)}{\sin\left(h\frac{\pi}{2l}\right)} \cos\left(h\frac{\pi}{4}\frac{l+1}{l}\right)$$

that is formula (11) which can be written as:

$$\frac{\sin\left(h\left(\frac{\pi}{4} - \frac{\pi}{4l}\right)\right)}{\sin\left(h\frac{\pi}{2l}\right)} \cos\left(h\left(\frac{\pi}{4} + \frac{\pi}{4l}\right)\right)$$

By using the goniometric formula $\sin p \cos q = \frac{1}{2}\left[\sin\left(q+p\right) - \sin\left(q-p\right)\right]$, the previous formula becomes:

$$\frac{1}{2}\frac{\sin\left(h\frac{\pi}{2}\right) - \sin\left(h\frac{\pi}{2l}\right)}{\sin\left(h\frac{\pi}{2l}\right)}$$

$$= \frac{1}{2}\left[\frac{\sin\left(h\frac{\pi}{2}\right)}{\sin\left(h\frac{\pi}{2l}\right)} - 1\right]$$

that is formula (12). By substituting $(n-1)$ and $(n+1)$ to h, formula (13) is obtained:

$$\sum_{k=1}^{s} \left[\cos\left(\left(n-1\right)k\alpha\right) - \cos\left(\left(n+1\right)k\alpha\right)\right] =$$
$$= S_l\left(n-1\right) - S_l\left(n+1\right) =$$
$$\frac{1}{2}\left[\frac{\sin\left((n-1)\frac{\pi}{2}\right)}{\sin\left((n-1)\frac{\pi}{2l}\right)} - \frac{\sin\left((n+1)\frac{\pi}{2}\right)}{\sin\left((n+1)\frac{\pi}{2l}\right)}\right]$$

Considering S as function in the variable n, by applying to the numerators the goniometric formula $\sin\left(q \pm p\right) = \sin p \cos q \pm \sin q \cos p$, previous formula becomes:

$$-\frac{1}{2}\cos n\frac{\pi}{2}\left[\frac{1}{\sin\left((n-1)\frac{\pi}{2l}\right)} + \frac{1}{\sin\left((n+1)\frac{\pi}{2l}\right)}\right]$$

$$= -\frac{1}{2}\cos n\frac{\pi}{2}\, \frac{\sin\left((n+1)\frac{\pi}{2l}\right) + \sin\left((n-1)\frac{\pi}{2l}\right)}{\sin\left((n-1)\frac{\pi}{2l}\right)\,\sin\left((n+1)\frac{\pi}{2l}\right)}$$

$$= -\cos n\frac{\pi}{2}\, \frac{\sin\left(n\frac{\pi}{2l}\right)\cos\left(\frac{\pi}{2l}\right)}{\sin\left((n-1)\frac{\pi}{2l}\right)\,\sin\left((n+1)\frac{\pi}{2l}\right)}$$

that is (14).

REFERENCES

[1] M. S.A. Dahidah, G. Konstantinou, and V.G. Agelidis, "A review of multilevel selective harmonic elimination PWM: formulations, solving algorithms, implementation and applications," *IEEE Trans. Power Electron.*, vol. 30, no. 8, pp. 4091-4106, Aug. 2015.

This article has been accepted for publication in a future issue of this journal, but has not been fully edited. Content may change prior to final publication. Citation information: DOI 10.1109/TPEL.2018.2878967, IEEE Transactions on Power Electronics

[2] H. Zhao, T. Jin, S. Wang, L. Sun, "A Real-Time Selective Harmonic Elimination Based on a Transient-Free Inner Closed-Loop Control for Cascaded Multilevel Inverters," *IEEE Trans. Power Electron.,* vol. 31, no. 2, pp. 1000-1014, Feb. 2016.

[3] R.P. Aguilera, P. Acuna, P. Lezana, G. Konstantinou, B. Wu, S. Bernet, V.G. Agelidis, "Selective Harmonic Elimination Model Predictive Control for Multilevel Power Converters," *IEEE Trans. Power Electron.,* vol. 32, no. 3, pp. 2416-2426, March 2017.

[4] E. Mohammadhossein, G. Negareh, V. Don Mahinda, L.M. Wynand, "Particle swarm optimisation-based modified SHE method for cascaded H-bridge multilevel inverters," *IET Power Electron.,* vol. 10, no. 1, pp. 18-28, 2017.

[5] P. L. Kamani and M.A. Mulla, "Middle-level SHE Pulse-Amplitude Modulation for Cascaded Multilevel Inverters," *IEEE Trans. Ind. Electron.,* vol. 65, no. 3, pp. 2828-2833, March 2018.

[6] M. Ahmed, A. Sheir, M. Orabi, "Real-Time Solution and Implementation of Selective Harmonic Elimination of Seven-Level Multilevel Inverter," *IEEE Journal of Emerg. and Select. Topics in Pow. Electron.,* vol. 5, no. 4, pp. 1700-1709, Dec. 2017.

[7] M. Hajizadeh, S.H. Fathi, "Selective harmonic elimination strategy for cascaded H-bridge five-level inverter with arbitrary power sharing among the cells," *IET Power Electron.*, vol. 9, no. 1, pp. 95-101, 2016.

[8] L.M. Tolbert, L.M., Chiasson, J.N., Du, Z., et al., "Elimination of harmonics in multilevel converter with nonequal DC sources," *IEEE Trans. Ind. Appl.,* vol. 41, no. 1, pp. 75-82, Jan./Feb. 2005.

[9] H. Taghizadeh and M. Tarafdar Hagh, "Harmonic Elimination of Cascade Multilevel Inverters with Nonequal DC Sources Using Particle Swarm Optimization," *IEEE Trans. Power Electron.*, vol. 57, no. 11, pp. 3678-3684, Nov. 2010.

[10] M.G. Hosseini Aghdam, S.H. Fathi, G.B. Gharehpetian, "Elimination of Harmonics in a Multi-Level Inverter with Unequal DC Sources Using the Homotopy Algorithm," *IEEE Int. Symp. on Ind. Electron., ISIE 2007*, pp. 578-583, 2007.

[11] L.K. Haw, M. S. A. Dahidah, H. A.F. Almurib, "SHE_PWM Cascaded Multilevel Inverter With Adjustable DC Voltage Levels Control for STATCOM Applications," *IEEE Trans. Power Electron.,* vol. 29, no. 12, pp. 6433-6444, Dec. 2014.

[12] C. Buccella, C. Cecati, M. G. Cimoroni, "Performance analysis and simulation of unbalanced DC sources five level inverter topology," *4th Int. Conf. on Renewable Energy Research and Applicat.*, *ICRERA 2015*, Palermo, Italy, pp. 1152-1156, 22-25 Nov. 2015.

[13] M. Najjar, A. Moeini, M.K. Bakhshizadeh, F. Blaabjerg and S. Farhangi, "Optimal Selective Harmonic Mitigation Technique on Variable DC Link Cascaded H-Bridge Converter to Meet Power Quality Standards," *IEEE Journal of Emerg. and Select. Topics in Pow. Electron.,* vol. 4, no. 3, pp. 1107-1116, Sept. 2016.

[14] M. Sharifzadeh, H. Vahedi, C. Cecati, C. Buccella, K. Al-Haddad, "A generalized formulation of SHM-PAM for cascaded H-bridge inverters with non-equal DC sources,"*IEEE Int. Conf. on Ind. Technology (ICIT17)*, pp. 18 - 23, Toronto, Canada, March 22-25, 2017.

[15] Z. Yuan, R. Yuan, W. Yu, J. Yuan, J. Wang, "A Groebner Bases Theory-Based Method for Selective Harmonic Elimination," *IEEE Trans. Power Electron.*, vol. 30, no. 12, pp. 6581-6592, Dec. 2015.

[16] K. Yang, Q. Zhang, R. Yuan, W. Yu, J. Yuan, J. Wang, "Selective Harmonic Elimination With Groebner Bases and Symmetric Polynomials," *IEEE Trans. Power Electron.* vol. 31, no. 4, pp. 2742-2752, Apr. 2016.

[17] C. Buccella, C. Cecati, M. G. Cimoroni, K. Razi, "Analytical method for pattern generation in five-level cascaded H-bridge inverter using selective harmonic elimination, " *IEEE Trans. Ind. Electron.,* vol. 61, no. 11, pp. 5811-5819, Nov. 2014.

[18] C. Buccella, C. Cecati, M. G. Cimoroni, G. Kulothungan, A. Edpuganti, A. Kumar Rathore, "A Selective Harmonic Elimination Method for Five-Level Converters for Distributed Generation," *IEEE Journal of Emerg. and Select. Topics in Pow. Electron.,* vol. 5, no. 2, pp. 775-783, June 2017.

[19] C. Buccella, M.G. Cimoroni, H. Latafat, G. Graditi, R. Yang, "Selective harmonic elimination in a seven level cascaded multilevel inverter based on graphical analysis," *IEEE Int. Conf. on Ind. Electron.(IECON16)*, pp. 2563-2568, Florence, Italy, Oct. 24-27, 2016.

[20] S.S. Lee, B. Chu, N.R.N. Idris, H.H. Goh, and Y.E. Heng, "Switched-battery boost-multilevel inverter with GA optimized SHEPWM for standalone application," *IEEE Trans. Ind. Electron.*, vol. 63, no. 4, pp. 2133-2142, April 2016.

[21] E. Suli and D.F. Mayers, *An Introduction to Numerical Analysis*, 1st ed. Cambridge, U.K.: Cambridge Univ. Press, 2003.

[22] https://www.digipower.it.

[23] DE10-Nano board, http://www.terasic.com.tw/cgi-bin/page/archive.pl?Language=English&CategoryNo=165&No=1046.

[24] Quartus Prime version 16.1.0, https://www.altera.com/products/design-software/fpga-design/quartus-prime/overview.html.

Concettina Buccella (M'92–SM"92–SM'03) received the M.S. degree in 1988 and the Ph.D. degree in Electrical Engineering in 1995 from the University of L"Aquila, Italy, and the University of Rome "La Sapienza", respectively. From 1988 till 1989 she has been a research engineer with Italtel SpA, L"Aquila. In 1991 she joined the Department of Electrical Engineering at the University of L"Aquila where since 2001 she is an Associate Professor in Electrotechnics. She holds three italian habilitations as Full Professor in Power Converters, Drivers, Machines and Power Systems and in Electrotechnics. Her research interests deal with smart grids, power converters modulation techniques, renewable energy management, analytical and numerical modeling. She has been a corecipient of the 2012 and th 2013 Best Paper Award of the *IEEE Transactions on Industrial Informatics*. She is an Associate Editor of the *IEEE Transactions on Industrial Electronics*, moreover she has been the Chair of the IEEE-IES Renewable Energy Systems Technical Committee from 2017 till 2018. She is the Chief Scientific Officer at DigiPower srl a R&D company active in the field of power electronics.

Maria Gabriella Cimoroni received the M.Sc. degree in Mathematics (summa cum laude) in 1989 from the University of L"Aquila. After graduation, she attended the post-graduate Inter-University Schoool in Perugia and the CNR Computational Mathematics School in Naples. Since 1994 she is a Researcher in Numerical Analysis at the University of L"Aquila. Her research activities deal with new spline operators for approximation of functions, for numerical evaluation of Cauchy principal value integrals and for numerical solution of integro-differential equations and since some years with analytical and numerical methods for modulation algorithms for multilevel converters. She has been a reviewer for several international conferences and *IEEE Transactions*. Prof. Cimoroni has been a Publication Chair of IEEE-IECON 2016 and the Publicity Chair of 5th International Symposium on Environment Friendly Energies and Application (EFEA 2018) in Rome.

Mario Tinari received the B.S. degree in Industrial Engineering and the M.S. degree in Electrical Engineering (with honors) from the University of L'Aquila, Italy, in 2014, and 2016, respectively. He is currently working toward the Ph.D. degree in Information Engineering, Computer Science and Mathematics at the University of L'Aquila, Italy. He is also a consultant with DigiPower srl, L'Aquila, Italy, a R&D company active in the field of power electronics. His current research interests includes modeling and design of power electronics circuits, efficient power conversion, renewable electrical energy systems, smart grids.

Carlo Cecati (M'90–SM'03–F"90–SM'03–F'06) received the Dr. Ing. Degree in Electrotechnical Engineering from the University of L'Aquila, L"Aquila, in 1983. Since then, he has been with the same university where he is a Professor of Industrial Electronics and Drives. From 2015 to 2017, he has been a Qianren Talents Professor (1000 Talents Program distinguished professor) with the Harbin Institute of Technology, Harbin, China. His research interests include power electronics, distributed generation, and smart grids. From 2013 to 2015 Prof. Cecati has been the Editor-in-Chief of the *IEEE Transactions on Industrial Electronics*. He has been a corecipient of the 2012 and the 2013 Best Paper Award from the *IEEE Transactions on Industrial Informatics* and of the 2012 Best Paper Award from the *IEEE Industrial Electronics Magazine*. In 2017 he received the Antony J. Hornfeck Award from the IEEE Indutrial Electronics Society. He is Chief Technical Officer at DigiPower srl a R&D company active in the field of power electronics.